IEEE Photonics Journal
An IEEE Photonics Society Publication

UV Plasmonic Structures: Direct Observations of UV Extraordinary Optical Transmission and Localized Field Enhancement Through Nanoslits

Volume 1, Number 4, October 2009

Qiaoqiang Gan
Liangcheng Zhou
Volkmar Dierolf
Filbert J. Bartoli

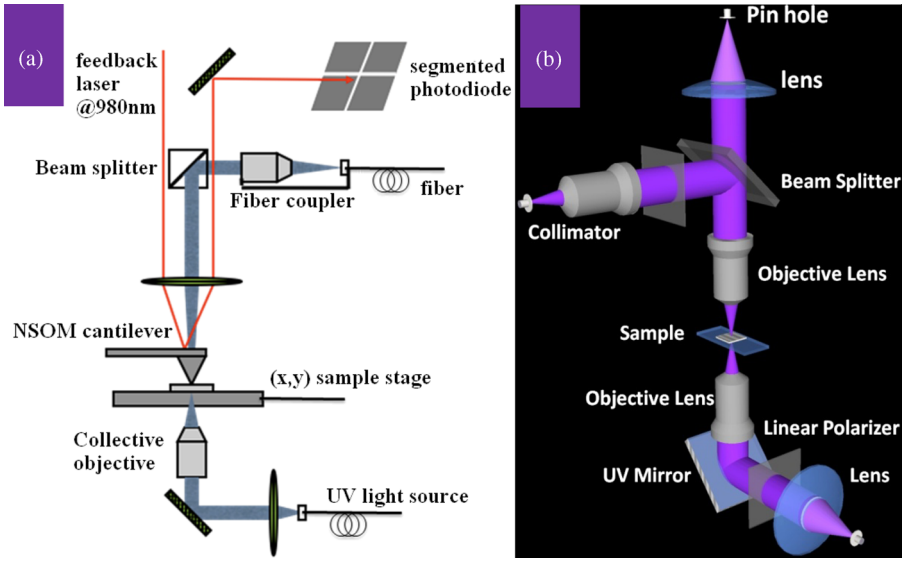

DOI: 10.1109/JPHOT.2009.2035998
1943-0655/$26.00 ©2009 IEEE

UV Plasmonic Structures: Direct Observations of UV Extraordinary Optical Transmission and Localized Field Enhancement Through Nanoslits

Qiaoqiang Gan, Liangcheng Zhou, Volkmar Dierolf, and Filbert J. Bartoli

Center for Optical Technologies, Lehigh University, Bethlehem PA 18015 USA

DOI: 10.1109/JPHOT.2009.2035998
1943-0655/$26.00 ©2009 IEEE

Manuscript received September 1, 2009; revised October 28, 2009. First published Online November 1, 2009. Current version published November 17, 2009. This work was supported by the National Science Foundation under Award ECS-0901324 and Award DMR-0602986. Corresponding author: Q. Gan (e-mail: qig206@lehigh.edu).

Abstract: The ultraviolet (UV) extraordinary optical transmission through nanoslit structures in the far field and the localized field enhancement in the near field are directly observed and compared with each other. Numerical modeling results are also presented, and the distribution properties of the UV Surface Plasmon polaritons (SPPs) are analyzed, showing agreement with the experiment results. These phenomena may enrich the studies on subwavelength optics on a chip and especially be useful for performance optimization of UV active devices, e.g., UV light-emitting diodes (LEDs) and UV detectors.

Index Terms: Surface Plasmon polariton, ultraviolet optics, extraordinary optical transmission.

1. Introduction

Surface Plasmon polaritons (SPPs) are of considerable interest for applications involving on-chip integration of optical circuits, data storage, and biosensing [1]–[6]. Since Ebbesen's report of *far-field (FF)* extraordinary optical transmission (EOT) through plasmonic hole arrays in 1998 [7], nanoplasmonics has become an area of intense interest, fueled in part by rapid advances in nanofabrication and nanocharacterization techniques. Researchers employed the SPP concept to design structures and devices with unique functionality or improved performance, in areas such as plasmonic waveguides [6], light emitting diodes (LEDs) [8], nanodetectors [9], solar cells [10], [11], planar collimators [12], [13], super lenses [14], etc. The primary focus of this work has been on SPPs in visible, near-infrared [1]–[3] and terahertz domains [15]–[17]. To date, there has been much less attention paid the properties of ultraviolet (UV) SPPs, although some groups reported measurements [18]–[22] or numerical simulations [23], [24] employing UV light to excite SPPs for *near-field (NF)* nanolithography [14]. They presented *NF* lithographic results on photo-resist layers as an indirect demonstration of subwavelength UV SPP distributions [18]–[22]. Recently, our group reported the direct mapping of the UV surface modes at the Al/Al_2O_3 interfaces [25]. However, no work has been reported that concurrently address the properties of plasmonic structures and UV device design, an area of research important to future progress in this spectral region.

UV semiconductor devices, such as UV LEDs and UV detectors, are important for nanofabrication (e.g., optical lithography) and a variety of other civil and military applications [26], [27]. For example, semiconductor UV light sources are needed for chemical and biological agent

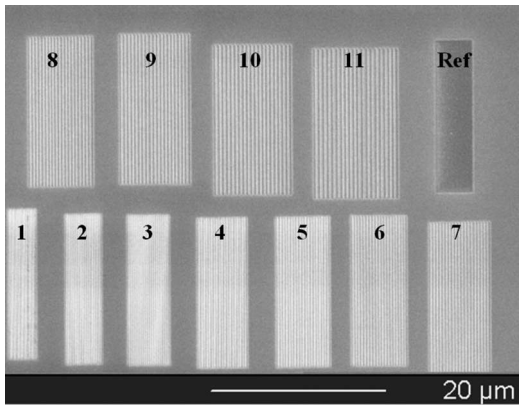

Fig. 1. SEM image of the samples. The parameters period (p) and width (w) of the gratings for all the samples are as follows: Sample 1 (p: 160 nm, w: 60 nm), sample 2 (p: 210 nm, w: 70 nm), sample 3 (p: 250 nm, w: 80 nm), sample 4 (p: 290 nm, w: 100 nm), sample 5 (p: 320 nm, w: 110 nm), sample 6 (p: 340 nm, w: 150 nm), sample 7 (p: 360 nm, w: 160 nm), sample 8 (p: 390 nm, w: 170 nm), sample 9 (p: 410 nm, w: 180 nm), sample 10 (p: 450 nm, w: 210 nm), and sample 11 (p: 500 nm, w: 220 nm). There are 20 slits in each array.

detection and efficient solid-state lighting [28]. The availability of chip-scale UV semiconductor LEDs [28]–[30] that could be focused to a spot size much less than the wavelength and are suitable for 2-D integration at these short wavelengths may open up new applications in fields such as information storage technology, environmental protection, and biomedicine. Equally important is the development of high-performance UV detectors that are required for solar UV monitoring, source calibration, UV astronomy, flame sensors and secure space-to-space communication [26], [27]. Performance improvements in such semiconductor devices are needed to enhance the external extraction efficiency for LEDs and coupling efficiency for detectors. In addition to the above, localized field enhancement (LFE) at UV wavelengths will be promising for novel on-chip UV light sources for biosensing and biomedical research. Before plasmonic structures can be employed to improve the performance of these devices in the UV domain, UV EOT as well as LFE have to be better understood and experimentally realized. This Letter presents, to our knowledge, the first direct observation of UV EOT through nanoslits in the FF and LFE in the NF. This represents an important step in the development of novel plasmonic structures for active UV devices, e.g., UV LEDs and UV detectors, and should also impact UV photonic applications in biosensing, bioimaging, and biomedicine.

2. Sample and Measurement System

We fabricated a series of nanograting structures with periods ranging from 160 nm (sample 1) to 500 nm (sample 11) using a focused-ion-beam (FIB) milling technique (FEI DB 235). The metal surface is a 50-nm-thick Al layer deposited on a 0.15-mm cover glass (Fisherbrand). Fig. 1 shows a scanning electron microscopy (SEM) image of all the samples on the Al layer. Sample 12 is a reference rectangular aperture with a size of 4.2 μm $\times$ 20 μm. The wavelength of the excitation beam is 364.7 nm in a vacuum (i.e., a wavelength in UV-A region).

We employ a NF scanning optical microscope (NSOM) equipped with a confocal microscope function to probe the transmission light signal through the Al nanoslits. The schematic diagram of the system is shown in the supplementary material for both NF [Fig. S1(a)] and FF [Fig. S1(b)] measurements. This instrument is a modified version of a commercial NSOM system (a-SNOM, WiTec GmbH, Germany). All of the optics in the system are UV compatible. For the NF observation, an Al cantilever probe with an aperture size of about 50 nm is used to collect photons above the Al surface. In this experiment, the tip is located at a constant height of about 10 nm above the sample. The confocal microscope is employed to observe the FF light signal, which is similar to the measurement in [31]. A 25-μm spatial filter aperture was placed at the focal plane to limit the FF

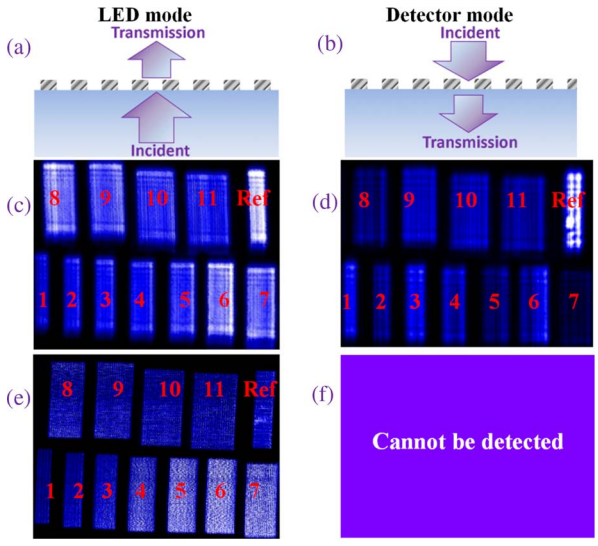

Fig. 2. Measurement results of the transmitted images through the nanoslit structures in the NF and FF. (a) and (b) Schematic diagrams for the LED mode and Detector mode, respectively. (c) and (d) Confocal microscope measurement results in the LED mode and Detector mode, respectively. (e) NSOM measurement result in the LED mode. (f) Blank because the NSOM probe cannot be placed at the metal/dielectrc interface in the Detector mode. In these measurements, the polarization direction of the incident light is perpendicular to the slit direction. The color bar is scaled to make the photos clear to the eyes. The data of the measurements are listed in Table 1.

transmission. In our measurement, all the samples are characterized in a single scan and their transmitted intensities are compared.

3. Measurement Design

It is known that only TM modes (where the electrical field of the incident light is perpendicular to the slits) could excite SPP modes on the grating structures, which will be discussed in detail below. Here, we define the following two measurement modes.

(1) LED mode: When the incident light propagates from the substrate to the metal structure, and is then radiated into the air, as shown in Fig. 2(a). This is similar to the case of coupling internally reflected light from LEDs out of the device. In this mode, the FF transmission could be observed using a confocal microscope [see Fig. 2(c)], and the NF distribution at the interface of metal/air could be observed by NSOM as shown in Fig. 2(e). (2) Detector mode: When the light propagates from the air to the metal structure and then is transmitted into the substrate, as shown in Fig. 2(b). This is similar to the case of enhanced coupling of the external light into the active detection region. In this mode, the FF transmitted light through all the samples could be observed using the confocal microscope as shown in Fig. 2(d). However, the NF distribution at the interface of metal/substrate cannot be detected because the tip cannot be placed at that interface [see Fig. 2(b) and (f)]. Measured values of the transmitted optical power, normalized to that of the reference, are listed in Table 1.

4. Discussion

(1) We will discuss the UV LED-mode measurement first [see Fig. 2(a)]. In this mode, values of the optical power transmitted through the nanoslits were directly measured in both the FF and the NF. The FF transmission signals observed using the confocal microscope are shown in Fig. 2(c) for each structure. It can be seen that the powers transmitted through samples 6–8 are stronger than those from the other samples [see the Normalized power data in column (I) in Table 1]. The transmission through the 11 samples, relative to that of the reference sample, varies from 49% to 96%. As seen in the transmission data in column (I) of Table 1, the maximum transmission was

TABLE 1

Measured Optical Transmission. P Is the Power Transmitted by Each Sample, Normalized to That of the Reference Sample (These Data Correspond to the Image Data in Fig. 2). W_s Is the Total Width of All the Slits in Each Structure, and W_{tot} Is the Total Width of Each Sample. The Total Sample Area Is $A_{tot} = W_{tot} \times L$, Where L Is 20 μm, $A_s = W_s \times L$ Is Net Area Occupied by the Slits, and A_{ref} Is the Area of the Reference Sample. The Transmission for Each Sample, Which Is Given by $P \times A_{ref}/A_{tot}$, Ranges From a Low of Approximately 0.49 for Sample 1 to a High of 0.96 for Sample 6. The Column of Normalized Intensity Is Obtained From $P \times A_{ref}/A_s$

	W_s (μm)	W_{tot} (μm)	(I) LED mode, Far field		(II) LED mode, NSOM		(III) Detector mode, Far field	
			Normalized transmitted power P	Normalized transmitted intensity	Normalized transmitted power P	Normalized transmitted intensity	Normalized transmitted power P	Normalized transmitted intensity
Ref	4.2	4.2	1	1	1	1	1	1
1	1.2	3.2	0.375	1.313	0.517	1.808	0.424	1.484
2	1.5	4.2	0.543	1.521	0.795	2.227	0.308	0.861
3	1.6	5.0	0.680	1.786	1.192	3.129	0.585	1.535
4	2.0	5.8	0.833	1.749	1.835	3.854	0.523	1.098
5	2.2	6.4	1.024	1.955	2.483	4.740	0.365	0.696
6	3.0	6.8	1.561	2.185	2.742	3.838	0.678	0.950
7	3.2	7.2	1.467	1.926	2.986	3.919	0.326	0.428
8	3.4	7.8	1.500	1.853	1.571	1.940	0.488	0.603
9	3.6	8.2	1.454	1.697	1.680	1.960	0.828	0.967
10	4.2	9.0	1.455	1.455	1.802	1.802	0.861	0.861
11	4.4	10	1.420	1.356	1.901	1.815	0.818	0.781

observed for sample 6, which has a period of 340 nm and the width of 150 nm. By comparing the transmitted intensities for the 11 samples to those for the reference sample, one can determine the transmitted intensity enhancement. As shown by the Normalized intensity data in column (I) of Table 1, the strongest intensity enhancement was observed for sample 6, i.e., approximately twice the incident intensity. This is clear evidence of EOT at this UV wavelength. Such Al nanoslit structures could be useful to enhance the external quantum efficiency of UV LEDs. In addition, it is believed that there are other potential advantages for using metallic slit arrays as they can act as electrodes to spread the electric current over the LED surface [32]: If the metallic nanoslit structure is employed as the interdigitated electrode for the LED, the current crowding effect could be optimized [33], [34] which is helpful to further improve the performance of the device. It is worth noting that SPPs were also employed to enhance the internal quantum efficiency of LEDs [8], [35], which is a logical next step in UV plasmonic studies but beyond the scope of this paper.

In recent years, researchers employed various theoretical models to investigate the physics of light transmission through subwavelength slits and slit arrays [36]. However, a number of physical issues are still not well understood, such as the transmission profile as a function of array period, interference between the SPPs and scattered light, the relation between the NF modes and the FF scattering, etc. To date, no measurements have been reported that compare the FF transmission to the NF distribution for the nanostructures. To explore this important relationship, we employed NSOM to probe the NF distribution for the same series of nanoslit arrays [see Fig. 2(e)]. The measured NF intensities for samples 4–7 are about four or five times that for the reference sample, suggesting that the LFE is achieved with these structures. As shown by the Normalized intensity data in column (II) of Table 1, the strongest NF intensity was observed for sample 5, which differs slightly from the FF results (discussed above) where sample 6 exhibited the highest intensity. It is recognized that the intensity distributions in the NF and FF can differ qualitatively. For instance, Table 1 shows that the NF intensity for sample 8 is weaker than those for samples 2–4, whereas the

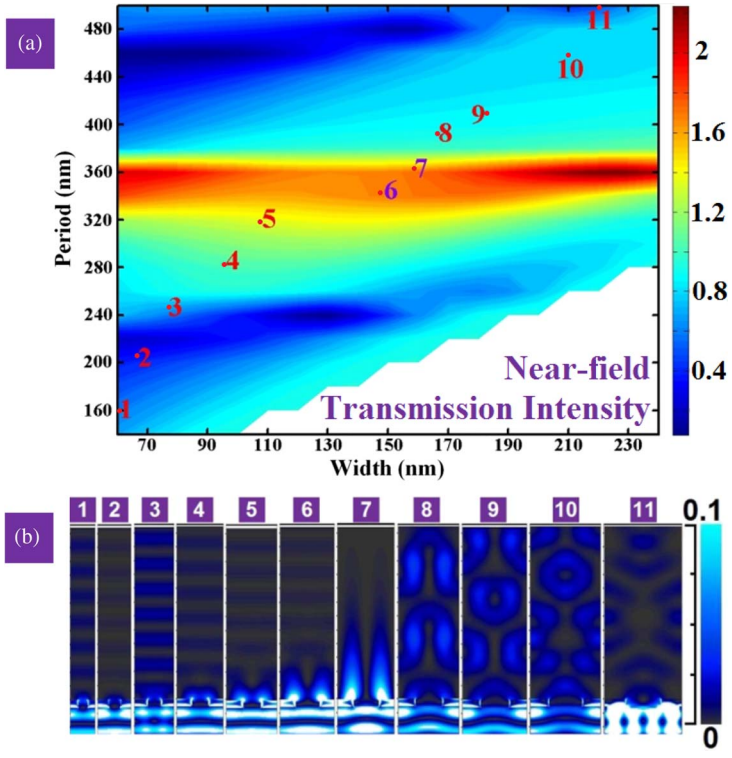

Fig. 3. (a) FDTD modeling of the transmitted intensities through the slits with various periods and widths in the NF (10 nm above the grating surface). (b) 2-D field distribution through the 11 samples in the LED mode. The space above the metal is the air, and the space under the metal is the glass substrate.

FF intensity for sample 8 is greater than those for samples 2–4 [see Fig. 2(c) and (e) and data in columns (I) and (II) in Table 1], suggesting that the radiation from the SPP modes to the propagating beam through samples 2–4 is not so effective. Considering the asymmetric structure of the glass/Al/air interface, no existing theoretical mechanisms can satisfactorily explain this difference between the field distributions in the NF and FF as well as the coupling from the SPPs to directional propagating beams in the free space [12], [13], [31], [36]–[38]. We believe that a direct experimental comparison of NF and FF intensity distributions, such as those reported here will provide new experimental data that may be instrumental in the development of a rigorous theoretical framework for understanding the optical behavior of the nanoslits. We also believe that these structures with LFE are beneficial to integrated UV light sources on a chip.

To numerically optimize plasmonic structures for LFE, we employ FDTD methods to model the UV intensities transmitted through the grating structures with various periods and slit widths in the NF (10 nm above the grating surface). The results are shown in Fig. 3(a). Field enhancement can be observed in the NF of samples 5–7, indicating that SPPs are excited effectively and lead to localized intensity enhancement. This is also illustrated in Fig. 3(b), which displays 2-D FDTD modeling results that are in reasonably good agreement with the experimental results in Fig. 2(e). These LFE observations could prove beneficial for future biosensing and bioimaging applications, and for integrated plasmonic light sources on a chip [39] in the UV domain. Based on the above observations and discussion, it should be clear that one has to properly design the structures using appropriate design rules to achieve EOT in the FF or LFE in the NF. However, it should be noted that for real LED devices, the light will be emitted over a wide range of angles. Current studies using normal incidence or relative small incident angles are just the first step along this direction. Further studies to quantitatively estimate the angular dependence of the transmission are still under investigation.

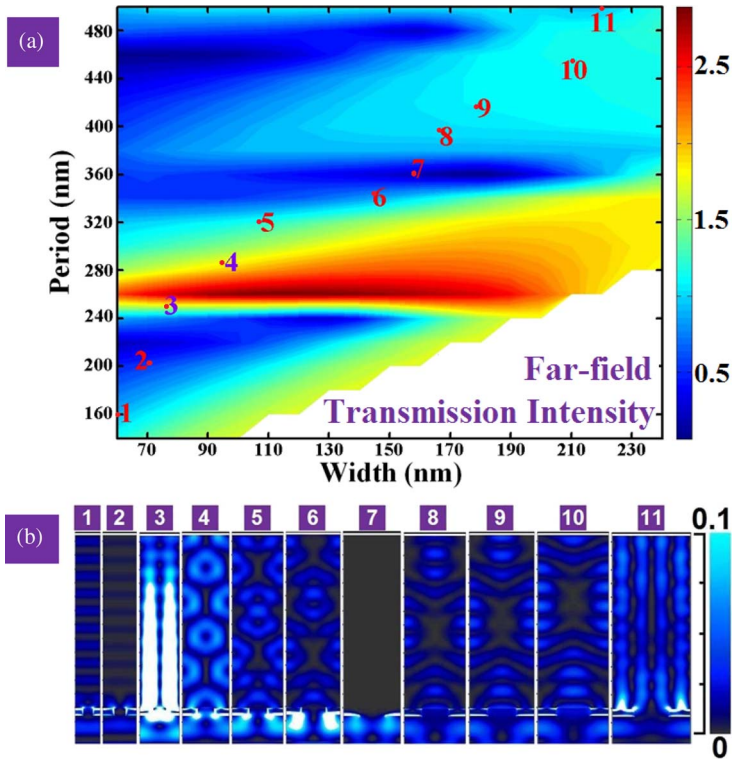

Fig. 4. (a) FDTD modeling of the FF transmitted intensity (1.15 μm above the grating surface) through the slits with various periods and widths. (b) 2-D field distribution through the 11 samples in the Detector mode. The space above the metal is the glass substrate, and the space under the metal is the air.

(2) We now discuss experimental and simulation results obtained for the Detector mode [see Fig. 2(b)]. While enhancement in coupling efficiency is an important goal for UV detector designs, as it is for the LED mode discussed above, high-speed response is also essential in some applications, especially for secure space-to-space communications. It is well known that the speed of photodiodes is primarily limited by two factors: the transit time of photogenerated carriers to the electrode and the depletion layer capacitance of the semiconductor [40]. Some groups employed interdigitated microelectrodes to cover the UV detector surface to reduce the transit time of photogenerated carriers to the electrodes [26], [41]. If the gap between the interdigitated electrodes is reduced to the nanometer scale, the speed of response could be improved significantly. However, the coupling efficiency was sacrificed when the detector aperture was partially covered. Consequently, realizing EOT through the nanoslit structures in the UV domain may be a promising means of overcoming this limitation and optimizing UV detector performance. Recently, the use of various nanoplasmonic structures was proposed by several groups to improve the performance of photodetectors at near-infrared wavelengths [42]–[45], further illustrating the potential benefit of plasmonic devices in optoelectronics.

In the Detector-mode experiments, only FF transmission through the nanoslits was measured [see Fig. 2(d)] since the NSOM tip cannot be placed directly at the metal/substrate interface. When the light propagates from air to the metal nanostructure and then into the substrate (in the opposite direction to that of the LED mode), one can see that the transmission through the 11 samples is unexpectedly different from that in the LED mode, indicating that a structure designed for a UV LED may not be equally useful for a UV detector. To our knowledge, such experimental results have not been reported previously, and could not be reliably predicted by the approximate theory for the transmission peak wavelength through nanoslit/hole arrays [46]. Researchers did realize that factors such as SPP interference and scattering loss have not been thoroughly considered in previous theories [1]–[3], [36], [47], suggesting that there is still much to be done to achieve a

detailed understanding of this phenomenon [36], [48], [49]. We note particularly that samples 5–7 do not have the strongest transmission in this Detector measurement mode. Sample 2 has a weaker transmission than samples 1 and 3, and sample 7 has the weakest of all 11 samples. The transmitted intensity through sample 3, which is the strongest among the 11 samples, is about 1.5 times that of the reference sample, indicating that EOT is observed in this FF measurement [see the data in column (III) in Table 1].

To understand this transmission data further, FDTD simulations are presented to model the transmitted intensities through the grating structures in the FF (1.15 μm above the grating surface): As shown in Fig. 4(a), samples 3 and 4 are close to the parameters providing the strongest transmission, while sample 7 is close to that for the weakest transmission. The optimized period is approximately 260 nm, where strong SPP modes could be excited at the glass substrate side. This is also illustrated by the field distribution simulation results in sample 3 in Fig. 4(b). The transmitted intensities through the 11 samples are in qualitative agreement with the measurement results in Fig. 2(d), although quantitative differences remain, for example, the FF transmission predicted for sample 1 is noticeably weaker than that for sample 3, whereas the experimental values are quite comparable (see column III in Table 1). Although NF distributions cannot be determined experimentally, they still can be simulated numerically as shown in Fig. 4(b). One can see that strong SPP enhancement can be achieved in sample 3, which is potentially useful for a light coupling enhancement window for novel UV detectors. If this structure is combined with interdigitated nanoelectrodes, the high coupling efficiency and high-speed response may be achieved simultaneously, which could have a great impact on future UV detector designs.

5. Conclusion

In summary, we have directly observed the UV EOT through nanoslit structures in the FF and LFE in the NF, respectively. The transmission is significantly different between the LED and the Detector modes for the same plasmonic structures, indicating that a rigorous framework for understanding the behavior of EOT through nanoplasmonic structures remains a significant scientific challenge. Investigations into these phenomena may enrich the studies on subwavelength optics on a chip and be especially important in the performance optimization of UV active devices. Numerical modeling results were also presented, and the distribution properties of the UV SPPs in the NF are analyzed, showing reasonable agreement with experiment, although some theoretical challenges remain. We believe that direct observations of the UV EOT and LFE have important implications for novel photonic applications in wide-bandgap semiconductor device design, optical integration, biosensing, bioimaging, and biomedicine [1]–[6] in the UV domain.

References

[1] W. L. Barnes, A. Dereux, and T. W. Ebbesen, "Surface plasmon subwavelength optics," *Nature*, vol. 424, no. 6950, pp. 824–830, Aug. 2003.
[2] E. Ozbay, "Plasmonics: Merging photonics and electronics at nanoscale dimensions," *Science*, vol. 311, no. 5758, pp. 189–193, Jan. 2006.
[3] C. Genet and T. W. Ebbesen, "Light in tiny holes," *Nature*, vol. 445, no. 7123, pp. 39–46, Jan. 2007.
[4] M. E. Stewart, C. R. Anderton, L. B. Thompson, J. Maria, S. K. Gray, J. A. Rogers, and R. G. Nuzzo, "Nanostructured plasmonic sensors," *Chem. Rev.*, vol. 108, no. 2, pp. 494–521, Feb. 2008.
[5] J. N. Anker, W. P. Hall, O. Lyandres, N. C. Shah, J. Zhao, and R. P. Van Duyne, "Biosensing with plasmonic nanosensors," *Nat. Mater.*, vol. 7, no. 6, pp. 442–453, Jun. 2008.
[6] S. Lal, S. Link, and N. J. Halas, "Nano-optics from sensing to waveguiding," *Nat. Photon.*, vol. 1, no. 11, pp. 641–648, Nov. 2007.
[7] T. W. Ebbesen, H. J. Lezec, H. F. Ghaemi, T. Thio, and P. A. Wolff, "Extraordinary optical transmission through subwavelength hole arrays," *Nature*, vol. 391, no. 6668, pp. 667–669, Feb. 1998.
[8] K. Okamoto, I. Niki, A. Shvartser, Y. Narukawa, T. Mukai, and A. Scherer, "Surface-plasmon-enhanced light emitters based on InGaN quantum wells," *Nat. Mater.*, vol. 3, no. 9, pp. 601–605, Sep. 2004.
[9] Y. Cui and S. He, "A theoretical re-examination of giant transmission of light through a metallic nano-slit surrounded with periodic grooves," *Opt. Express*, vol. 17, no. 16, pp. 13 995–14 000, Aug. 2009.
[10] S. Pillai, K. R. Catchpole, T. Trupke, and M. A. Green, "Surface plasmon enhanced silicon solar cells," *J. Appl. Phys.*, vol. 101, no. 9, p. 093 105, May 2007.

[11] V. E. Ferry, L. A. Sweatlock, D. Pacifici, and H. A. Atwater, "Plasmonic nanostructure design for efficient light coupling into solar cells," *Nano Lett.*, vol. 8, no. 12, pp. 4391–4397, Dec. 2008.
[12] N. Yu, J. Fan, Q. Wang, C. Pflügl, L. Diehl, T. Edamura, M. Yamanishi, H. Kan, and F. Capasso, "Small-divergence semiconductor lasers by plasmonic collimation," *Nat. Photon.*, vol. 2, no. 9, pp. 564–570, Sep. 2008.
[13] N. Yu, R. Blanchard, J. Fan, F. Capasso, T. Edamura, M. Yamanishi, and H. Kan, "Small divergence edge-emitting semiconductor lasers with two-dimensional plasmonic collimators," *Appl. Phys. Lett.*, vol. 93, no. 18, p. 181 101, Nov. 2008.
[14] X. Zhang and Z. Liu, "Superlenses to overcome the diffraction limit," *Nat. Mater.*, vol. 7, no. 6, pp. 435–441, Jun. 2008.
[15] S. Maier, S. R. Andrews, L. Martín-Moreno, and F. J. García-Vidal, "Terahertz surface plasmon-polariton propagation and focusing on periodically corrugated metal wires," *Phys. Rev. Lett.*, vol. 97, no. 17, p. 176 805, Oct. 2006.
[16] Q. Gan, Z. Fu, Y. Ding, and F. Bartoli, "Ultrawide-bandwidth slow-light system based on THz plasmonic graded metallic grating structures," *Phys. Rev. Lett.*, vol. 100, no. 25, p. 256 803, Jun. 2008.
[17] Q. Gan, Z. Fu, Y. Ding, and F. Bartoli, "Bidirectional subwavelength slit splitter for THz surface plasmons," *Opt. Express*, vol. 15, no. 26, pp. 18 050–18 055, Dec. 2007.
[18] W. Srituravanich, N. Fang, C. Sun, Q. Luo, and X. Zhang, "Plasmonic nanolithography," *Nano Lett.*, vol. 4, no. 6, pp. 1085–1088, Jun. 2004.
[19] N. Fang, H. Lee, C. Sun, and X. Zhang, "Sub–diffraction-limited optical imaging with a silver superlens," *Science*, vol. 308, no. 5721, pp. 534–537, Apr. 2005.
[20] D. B. Shao and S. C. Chen, "Surface-plasmon-assisted nanoscale photolithography by polarized light," *Appl. Phys. Lett.*, vol. 86, no. 25, p. 253 107, Jun. 2005.
[21] L. Wang, S. M. Uppuluri, E. X. Jin, and X. Xu, "Nanolithography using high transmission nanoscale bowtie apertures," *Nano Lett.*, vol. 6, no. 3, pp. 361–364, Mar. 2006.
[22] Z. Liu, Y. Wang, J. Yao, H. Lee, W. Srituravanich, and X. Zhang, "Broad band two-dimensional manipulation of surface plasmons," *Nano Lett.*, vol. 9, no. 1, pp. 462–466, Jan. 2009.
[23] Z. Liu, Q. Wei, and X. Zhang, "Surface plasmon interference nanolithography," *Nano Lett.*, vol. 5, no. 5, pp. 957–961, May 2005.
[24] D. B. Shao and S. C. Chen, "Numerical simulation of surface-plasmon-assisted nanolithography," *Opt. Exp.*, vol. 13, no. 18, pp. 6964–6973, Sep. 2005.
[25] Q. Gan, L. Zhou, V. Dierolf, and F. Bartoli, "Direct mapping of the UV surface plasmons," *Opt. Lett.*, vol. 34, no. 9, pp. 1324–1326, Apr. 2009.
[26] E. Munoz, E. Monroy, J. L. Pau, F. Calle, F. Omnes, and P. Gibart, "III nitrides and UV detectors," *J. Phys., Condens. Matter*, vol. 13, no. 32, pp. 7115–7137, 2001.
[27] E. Monroy, F. Omnes, and F. Calle, "Wide-bandgap semiconductor ultraviolet photodetectors," *Semicond. Sci. Technol.*, vol. 18, no. 4, pp. R33–R51, Mar. 2003.
[28] A. Khan, K. Balakrishnan, and T. Katona, "Ultraviolet light-emitting diodes based on group three nitrides," *Nat. Photon.*, vol. 2, no. 2, pp. 77–84, 2008.
[29] Y. Taniyasu, M. Kasu, and T. Makimoto, "An aluminium nitride light-emitting diode with a wavelength of 210 nanometres," *Nature*, vol. 441, no. 7091, pp. 325–328, May 2006.
[30] H. Matsubara, S. Yoshimoto, H. Saito, J. Yue, Y. Tanaka, and S. Noda, "GaN photonic-crystal surface-emitting laser at blue-violet wavelengths," *Science*, vol. 319, no. 5862, pp. 445–447, Jan. 2008.
[31] L. Verslegers, P. Catrysse, Z. Yu, J. White, E. Barnard, M. Brongersma, and S. Fan, "Planar lenses based on nanoscale slit arrays in a metallic film," *Nano Lett.*, vol. 9, no. 1, pp. 235–238, Jan. 2009.
[32] A. Drezet, F. Przybilla, E. Laux, O. Mahboub, C. Genet, T. W. Ebbesen, J. S. Bouillard, A. Zayats, I. S. Spevak, A. V. Zayats, A. Yu Nikitin, and L. Martín-Moreno, "Opening the light extraction cone of high index substrates with plasmonic gratings: Light emitting diode applications," *Appl. Phys. Lett.*, vol. 95, no. 6, p. 021 101, Aug. 2009.
[33] X. Guo and E. F. Schubert, "Current crowding in GaN/InGaN light emitting diodes on insulating substrates," *J. Appl. Phys*, vol. 90, no. 8, pp. 4191–4195, Oct. 2001.
[34] X. Guo and E. F. Schubert, "Current crowding and optical saturation effects in GaN/InGaN light-emitting diodes grown on insulating substrates," *Appl. Phys. Lett.*, vol. 78, no. 21, p. 3337, May 2001.
[35] K. Okamoto, I. Niki, A. Scherer, Y. Narukawa, T. Mukai, and Y. Kawakami, "Surface plasmon enhanced spontaneous emission rate of InGaN/GaN quantum wells probed by time-resolved photoluminescence spectroscopy," *Appl. Phys. Lett.*, vol. 87, no. 7, p. 071 102, 2005.
[36] J. Weiner, "The physics of light transmission through subwavelength apertures and aperture arrays," *Rep. Prog. Phys.*, vol. 72, no. 6, p. 064 401, May 2009.
[37] Q. Cao and P. Lalanne, "Negative role of surface plasmons in the transmission of metallic gratings with very narrow slits," *Phys. Rev. Lett.*, vol. 88, no. 5, p. 057 403, Feb. 2002.
[38] Y. Xie, A. Zakharian, J. Moloney, and M. Mansuripur, "Transmission of light through a periodic array of slits in a thick metallic film," *Opt. Exp.*, vol. 13, no. 12, p. 4485, Jun. 2005.
[39] D. M. Koller, A. Hohenau, H. Ditlbacher, N. Galler, F. Reil, F. R. Aussenegg, A. Leitner, E. J. W. List, and J. R. Krenn, "Organic plasmon-emitting diode," *Nat. Photon.*, vol. 2, no. 11, pp. 684–687, Nov. 2008.
[40] S. Donati, *Photodetectors*. Englewood Cliffs, NJ: Prentice-Hall, 2000.
[41] M. Liao, J. Alvarez, M. Imura, and Y. Koide, "Submicron metal-semiconductor-metal diamond photodiodes toward improving the responsivity," *Appl. Phys. Lett.*, vol. 91, no. 16, p. 163 510, Oct. 2007.
[42] T. Ishi, J. Fujikata, K. Makita, T. Baba, and K. Ohashi, "Si nano-photodiode with a surface plasmon antenna," *Jpn. J. Appl. Phys.*, vol. 44, no. 12, pp. L364–L366, Mar. 2005.
[43] L. Tang, D. Miller, A. Okyay, J. Matteo, Y. Yuen, K. Saraswat, and L. Hesselink, "C-shaped nanoaperture-enhanced germanium photodetector," *Opt. Lett.*, vol. 31, no. 10, pp. 1519–1521, May 2006.
[44] J. Hetterich, G. Bastian, N. Gippius, S. Tikhodeev, G. von Plessen, and U. Lemmer, "Optimized design of plasmonic MSM photodetector," *IEEE J. Quantum Electron.*, vol. 43, no. 10, pp. 855–859, Oct. 2007.

[45] J. Shackleford, R. Grote, M. Currie, J. Spanier, and B. Nabet, "Integrated plasmonic lens photodetector," *Appl. Phys. Lett.*, vol. 94, no. 8, p. 083 501, Feb. 2009.
[46] H. F. Ghaemi, T. Thio, D. E. Grupp, T. W. Ebbesen, and H. J. Lezec, "Surface plasmons enhance optical transmission through subwavelength holes," *Phys. Rev. B, Condens. Matter*, vol. 58, no. 11, pp. 6779–6782, Sep. 1998.
[47] T. D. Visser, "Surface plasmon at work?" *Nat. Phys.*, vol. 2, p. 509, 2006.
[48] F. J. García de Abajo, "Light scattering by particle and hole arrays," *Rev. Mod. Phys.*, vol. 79, no. 4, p. 1267, Oct. 2007.
[49] H. Liu and P. Lalanne, "Microscopic theory of the extraordinary optical transmission," *Nature*, vol. 452, no. 7188, pp. 728–731, Apr. 2008.